Long-term Effects of Drainage and Rewetting on the Degradation and Preservation of Peat Organic Matter in Warm Climate

Guy Sapir[1,2,3], Alon Angert[1], Yoav Oved Rosenberg[2], Rotem Golan[3].

[1] The Institute of Earth Sciences, The Hebrew University of Jerusalem, Israel. [2] Geological Survey of Israel, Jerusalem, Israel.

[3] Institute of Soil, Water and Environmental Sciences. Volcani Institute, Agricultural Research Organization, Israel.

Correspondence to: Alon Angert (angert@huji.ac.il)

Abstract. Peatlands cover about 3% of the earth's land surface, while storing about 20% of the total global soil organic carbon. These carbon stocks are largely at risk as many peatlands have deteriorated since the Industrial Revolution due to conversion to agricultural land by drainage. Globally, peatland drainage is responsible for over 3.5% of anthropogenic greenhouse gas emissions. About 75% of these emissions originate from warm climate regions. Mitigation of these emissions can be achieved by rewetting degraded peatlands. This study focuses on a warm-climate peatland that has been cultivated for the past ~70 years (Hula Valley, Israel). The historic marsh was drained in 1957 for agricultural use and underwent a hydrological restoration project for elevating and stabilizing groundwater table since 1994. This land management history resulted in a sedimentary peat column that can be divided into three distinct sub-sections: drained, rewetted and pristine peat. This setting enables studying the drainage and rewetting effects on soil organic matter (SOM) degradation and preservation under warm climates. For this purpose, five sediment cores, 4 m long each, were excavated from cropland located over the historic marsh area. Locations were chosen to match previous studies on this site. Each soil profile was characterized using Rock-Eval® thermal analysis of the organic matter, and short-term soil aerobic respiration experiments. Integration of these results with historic SOM content data and with SOM modelling was used to explore the long-term process and rate of degradation. We found that the mean SOM content in the top one meter of the soil profile declined from 68 ±4 wt.% to 21 ±2 wt.% over the past 66 years, excluding compaction effect. In comparison to the drained section, the rewetted and pristine sub-sections has a mean SOM of 33 ±2 wt.% and 64 ±2 wt.%, respectively. A peak in pyrite concentration beneath the recent water table-level, was observed in most profiles, indicating anaerobic conditions and sulfur recycling. Rock-Eval® thermal analysis demonstrated that during decomposition, the residual SOM became more oxidized and contained a lower proportion of thermally labile SOM, with a significant difference found between drained and rewetted peat. These results imply that the raising of the water table (~30 years ago) effectively helped preserving organic matter compared to the

30   drained section. Long-term SOM field data were integrated and studied using an SOM decomposition model and by incorporating respiration fluxes. The resulting trends highlighted that the first few decades of exposure are highly significant for the fate of the carbon stock, leading to substantial CO_2 emissions. These emissions were lower by 60–85% after 70 years. Furthermore, our results suggest that currently, approximately 13-21 wt.% of SOM persists as resistant organic matter in the degraded peat.

1   Introduction

Peatlands cover about 3% of the earth's land surface and estimated to store between 500-700 Pg of carbon (C), which are about 20% of the global total soil organic stock (Page et al., 2016). Peatland has been exploited intensively by humans since the Industrial Revolution. At present, human activity of draining and mining affects approximately 10% of the remaining global peatlands, transforming these ecosystems from long-term carbon

40   sinks into significant sources of greenhouse gases (GHG's) (Leifeld & Menichetti, 2018). This transformation promotes carbon loss, primarily through microbial respiration and dissolved organic carbon (DOC) leaching (Hiraishi et al., 2013). Degraded peatlands currently contain 80.8 Pg of carbon and 2.3 Pg of nitrogen (Leifeld & Menichetti, 2018). Without further protective actions, drained peatlands will release most of this stock as greenhouse gases into the atmosphere.

45   The primary factor that contributes to the preservation of peat organic matter (OM) is anaerobic conditions, which predominantly prevail in water-saturated conditions (Moore et al., 1989). In such environments, where the SOM supply rate exceeds the decomposition rate, a net carbon sink can evolve (Moore, 1989). Generally, organic matter is added to the surface of the mire (peat forming habitat) mainly from net primary production, and its accumulation is countered by decomposition processes. Decomposition in the top layer occurs under aerobic

50   conditions, followed by deeper burial in the saturated horizon where oxygen is limited (Moore 1989; Joosten, 2002). There, under anaerobic conditions, decomposition occurs at rates that are approximately a thousand times lower than the upper aerobic layer (Clymo et al., 1998; Kleinen et al., 2012). This low decomposition rates result in a carbon sink with a turnover time of several thousands of years if remains undisturbed (Yu et al., 2010). Lowering the water table level (WTL) results in oxidation of the peat column, stimulating aerobic microbial

55   decomposition of the SOM (Scanlon et al., 2000; Joosten, 2002), which releases intense CO_2 and N_2O fluxes into the atmosphere (Page et al., 2016). Draining peatlands by lowering the WTL to convert them into agricultural lands has been a widespread practice for centuries and continues today. Numerous studies, e.g., Hooijer et al. (2010) and Moore et al. (1989), have demonstrated a clear correlation between low WTL and high CO_2 emissions

due to peat soil respiration. Currently, more than 90% of global drained peatlands are used for agriculture

60   (Tubiello et al., 2016). This practice occurs across most climate zones, with the largest emissions rates from drained peatland are currently in Southeast Asia (Hooijer et al., 2010; Tubiello et al., 2016). Emissions rates due to microbial respiration are strongly controlled by temperature and therefore by climate zones. Drained peatlands in tropical regions have the highest annual emissions per area (~ 70-ton CO_2 ha^{-1} yr^{-1}) which is four and two times higher than in boreal and warm temperate climate zones, respectively (Tubiello et al., 2016, Hiraishi et al., 2013).

65   Global emissions stemming from drained peatlands are estimated to be ~1.9 Pg CO_2-eq yr^{-1} (Leifeld & Menichetti, 2018), accounting for ~3.6% of global anthropogenic CO_2-eq emissions, with ~77% of those emissions coming from tropical climate zone (Leifeld & Menichetti, 2018).

Peatland restoration, primarily through rewetting drained peat, can reduce global CO_2 emissions by 0.5-1.3 Pg CO_2-eq yr^{-1} (Leifeld and Menichetti, 2018; Gunther et al., 2020), and account for 30% of global mitigation

70   solutions for forests and other land ecosystems (Roe et al., 2021). Successful rewetting often involves blocking drainage systems, stabilizing water levels, and re-establishing vegetation adapted to wet conditions (Convention on Wetlands. 2021). While drainage leads to high CO_2 emissions, maintaining a high WTL can result in increased methane emissions. However, studies showed that raising the WTL to near the surface results in a net reduction of CO_2 emissions that outweighs methane emissions (Gunther et al., 2020; Wilson et al., 2016; Nyberg et al.,

75   2022). A global meta-analysis found that keeping the groundwater level close to the surface can reduce global GHG's emissions from wetlands by about 90% by the end of the 21st century (Zou et al., 2022). Despite many studies highlighting the importance of rewetting for climate mitigation, there is scarce data on organic matter preservation in rewetted tropical peatlands (Nabuurs et al., 2023; Wilson et al., 2016). Available data on rewetted sites are limited for several to ten years (Wilson et al., 2016), thus limiting the evaluation of rewetting effect on

80   SOC preservation and GHG's emissions. Moreover, information about the time-frame since drainage, during which rewetting is effective, is crucial for selecting sites for management and preservation actions.

Peatlands deposits are rich in organic matter, characterized by about 50 wt.% SOM (Joosten, 2002). While drainage leads to SOM loss and mineralization, studies have shown that recalcitrant material in peatlands may influence decomposition rates after drainage (Leifeld et al., 2012). Leifeld et al. (2012) showed that, in drained

85   peatlands, high respiration rates were correlated with high concentrations of O-alkyl-C (a functional group of labile compounds). Könönen et al. (2016) found that tropical peat drainage leads to an increase in recalcitrant compounds concentrations such as lignin. Phenol oxidase is known as a key factor in accelerating the decomposition of recalcitrant SOM such as lignin after drainage (Freeman et al., 2004). However, Fe(II) oxidation may inhibit phenol oxidase activity and further enhancing Fe(III) and lignin complexation, as suggested

90 by the 'iron gate' mechanism (Wang et al., 2017). These studies attest that the reactivity for decomposition depends on the different fractions and compounds of the SOM in peat. However, the fate of these recalcitrant compounds after prolonged peat degradation and mineralization is yet unknown.

Recent evidence in mineral soils studies suggests that stabilization by recalcitrant material, as proposed in the 'selective preservation' hypothesis, is not common and relevant only at the beginning of SOM decomposition and

95 in rich SOM soils (Rowley et al., 2017). Beside the limitations of oxygen availability due to water-saturation, and extreme temperature constraints on bacterial and enzymatic activity (Rowley et al., 2017), the most significant preservation mechanisms in mineral soils are SOM aggregation and mineral sorption (Lützow et al., 2006; Kleber et al., 2015). SOM aggregation is a physical process by which SOM is separated from decomposers by occluded organic and inorganic particles aggregate with cementing agents (Six et al. 2002). Aggregation is known to be

100 promoted both by microbial activity (Chenu and Cosentino, 2011) and inorganic components in the soil matrix (Vitro et al., 2013). The sorption mechanism involves a wide range of reactions between organic compounds and soil minerals. Various clay minerals, oxides, and cations exhibit a high affinity for bonding with organic matter, leading to stabilization (Kleber et al., 2015; Rowley et al., 2017). Recent studies indicate that microbial residue, known as necromass, and depolymerized organic compounds produced by microbes are highly correlated with

105 mineral-bonded OM, more than complex recalcitrant plant-derived material (Liang et al., 2017; Manzoni & Francesca, 2024).

Pristine peatlands lack these mechanisms (i.e., aggregation and sorption) due to their low mineral content (Leifeld et al., 2012; Mirabito & Chambers. 2023). However, these preservation mechanisms may become relevant after prolonged mineralization of peat soils. Limited knowledge exists about SOM pools and stabilization mechanism

110 in degraded peat soils. Thus, making it challenging to accurately characterize long-term peat degradation and select suitable models for describing peat SOM loss over time.

To the best of our knowledge, no long-term data or models on peat decomposition are available in the literature, although many studies have been conducted on mineral soils. For instance, multiple long-term Bare Fallow experiments, spanning several decades, have been conducted on mineral soils in cold temperate climate zones

115 (Barre et al., 2010). These experiments are especially valuable for identifying stable SOM, as they exclude organic matter inputs to the soil - a condition resembling drained peat.

Here we study a peatland site located in the Hula Valley, Israel, which has several important characteristics: (1) The site is located in a warm, subtropical climate; (2) The peat drainage occurred nearly 70 years ago, initiating a peat degradation period; (3) A rewetting of the bottom part of the degraded peat column, occurred three decades

120 ago, and left the upper peat column drained until present time; and (4) Numerous historical studies were conducted in this site, enabling long-term (66 years) tracking of SOM stock. This research hat two main objectives: First, to evaluate the long-term effect of rewetting on SOM preservation after nearly four decades of drainage in a warm climate. Second, to examine the decomposition rate of nearly 70 years long-term degradation of drained peat and to explore the fate of peat SOM after prolonged mineralization. To achieve this, we integrate

125 Rock-Eval analysis, short-term respiration experiments, historical geochemical data, and a SOM decomposition model to investigate the long-term effects of drainage and rewetting on SOM degradation and preservation in the Hula Valley peatland.

2   Study site

The Hula Valley, Israel (33.1°N, 35.6°E), spans 175 km², of which 28 km² consists of drained marshland that

130 accumulated peat, now used mostly as cropland. The basin sustained lacustrine environments for the past 4 million years (Bein, 1986), with the last Hula Marsh prevailing from 2.5 to 4 thousand years ago until its drainage in 1957 (Cowgill, 1969; Bein, 1986). The dominant species found in the accumulated peat soil of the historic marsh was Cyperus Papyrus (Bein and Horowitz, 1986). The peat has accumulated in the top section of the sediment, reaching up to 12 meters of peat at its central area (Bein, 1967). This central area is also known as the

135 'deep peat' area which spans 12 km² (Marish, 1986). In 1957, the Hula Marsh and Lake were drained, primarily for agricultural land use and of reduction of water loss through evaporation. Consequently, the habitat was destroyed, and the exposed peat underwent aerobic conditions, accelerating SOM oxidation in the following years. This led to spontaneous peat fires, erosion, soil loss, subsidence, and nutrient leaching into downstream waterways (Hambright and Zohary 1998; Litaor et al., 2011). In 1994, a major agricultural peat land preservation

140 project was initiated, in which partial rewetting was implemented to halt soil degradation and fires by means of raising and stabilizing the WTL and frequent irrigation of crops (Hambright and Zohary, 1998). Since then, the water table is managed at approximately -100 cm (Tsipris et al., 2021). Hence, the Hula's deep peat area can be divided vertically into 3 sections: (1) The deep pristine peat section (that was not drained) (2) mid-section of peat drained for 37 years (1957-1994) and then rewetted for the last 30 years (1994-present) and (3) the top peat

145 which was drained over the last 66 years (1957- present). The ambient air annual mean temperature is ~20°C (Marish, 1986; online data MIGAL, 2023), which classifies the area as a tropical soil respiration zone (Bond-Lamberty et al., 2024). Soil average daily temperature measured at -20 cm depth was ~30°C in summer months (Jun-Oct 2023) and ~15°C in winter months (Dec-Mar 2023), with annual mean of ~22°C (online data MIGAL,

2023). The annual mean precipitation was 610 mm (1987-97; Tsipris and Meron, 1998), and the peat area is used

150 for cropland which is regularly irrigated during summer months preventing the upper peat from drying. WTL are routinely measured in 19 observation wells and 4 operational drainage channels throughout the Hula Valley, as documented in MIGAL's multi-annual reports over the past 20 years (Tsipris et al., 2021). However, assessing WTL in the drainage period between 1957 and 1994, is more challenging due to limited data availability. To address this, we relied on historical studies. Yaari et al. (1971b) provides WTL data from core samples collected

155 in December 1970, specifying the WTL for each core (Table 1). A report by Marish (1986) presents a spatial WTL map for winter 1985, indicating areas where the WTL is above or below -120 cm, and notes that no significant changes in WTL have occurred since Yaari et al. (1971b) (Table 1). Therefore, we adopted Yaari et al. (1971b) WTL data to represent the period from post-drainage (1957) until the rewetting in 1994. Further, we choose to follow Yaari et al. (1971b) soil profile's locations for our study and soil core samples collection for

160 comparison. Table 1 presents the complete dataset of WTL variations from 1957 to 2021 in our examined profiles.

Table 1. water table levels in cm (-) for below ground surface			
Profile	**Yaari et al. (1971b)**	**Marish (1986)**	**Monitoring** (2001-2021) mean by annual (±STDV)
A*	-80	Above -120	-101 ± 18*
C	-220	Below -120	-226 ± 17
D*	-120	Above -120	-101 ± 18*
E*	-165	Below -120	-101 ± 18*
F	-200	Below -120	-95 ± 10

* Based on data collected from observation well number 13. Locations marked in Figure 1.

2.1   Sample collection

Soil samples were collected in January-April of 2023 from the 'Deep Peat' area (Fig. 1). Five different locations were chosen based on the sampling locations of Yaari et al. (1971a) designated there as Crossline B. For

175 coordinates, see the Supplementary Material (1.8). To ensure that the sampling will include the pristine peat, each core was excavated to a depth of approximately -400 cm (much deeper than the WTL preceding the drainage; Table 1). We used a manual gauge auger (Eijkelkamp©) of either 1 or 0.5 m long cores and of 5 and 2 cm diameter, respectively. The soil sampling from the cores was based on two collection schemes: (1) sampling of

discrete 2-5 gr sample, collected at 10 cm intervals, into pre-weighed 50 ml tubes. These samples were mainly
180   used for RockEval analysis, (2) sampling of homogeneous soil sections, based on lithology and historic WTL, at
30-60 cm intervals to cotton aired bags. These samples were mainly used for respiration incubation experiments.
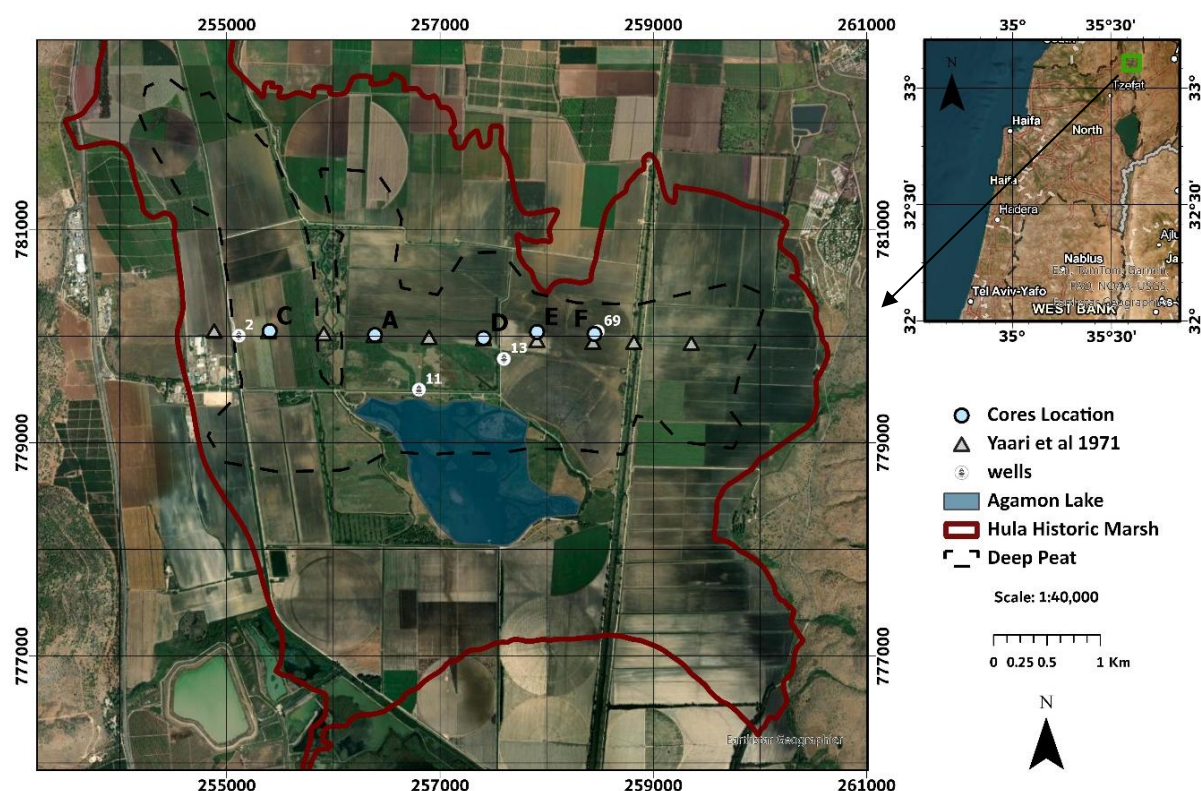

Figure 1: Study site satellite map – Hula valley, Israel (coordinates of Israel TM Grid). Polygons of the historic marsh boundaries in dark red, deep peat area in black dashed line (by Marish 1986), WTL observation wells in white circles, core locations in light blue. Regional map to the right in WGS 1984 coordinates. This image was made by ArcGIS software and is based on ESRI-provided data.

3   Materials and Methods

3.1   Rock-Eval Analysis

185   Analysis of the soil samples for SOM characterization was carried out with the newest Rock-Eval 7S analyzer
(RE-7S, Vinci Technologies). 107 samples of peat from all profiles were freeze-dried, ground, and homogenized
for analysis. About 15-30 mg of ground sample were taken for analysis. The analytical protocol included two

phases: (1) pyrolysis in an inert N_2 atmosphere starting at a temperature of 200 °C reaching 650 °C; (2) combustion using air, starting at a temperature of 300°C and rising to 850 or 1200°C when sulfates were also

190   quantified (see below). Both steps heating rate is 25 °C/min, and combustion had a final time of 10 min at maximum temperature before cooling down. The heating cycle is based on Behar et al. (2001) and modified for soils based on Sebag et al. (2016). The gradual heating of the RE-7S promotes a sequential decomposition of organic and inorganic phases according to their thermal stability. Continuous monitoring of the generated products is carried via four different detectors: (1) a Flame Ionization detector (FID) for hydrocarbons (HC), (2)

195   two Infrared (IR) detectors for CO and CO_2 and (3) Ultra violate (UV) detector for SO_2.

Calibration of C was done using the IFP 160000 standard (Behar et al., 2001). As carbonates are also decomposed during a RE analysis, an empirical separation between organic and inorganic C was previously determined for rocks and mineral soils (Behar et al. 2001). Usually, the organic CO, and CO_2 at the pyrolysis phase is determined up to 400°C, and for the oxidation phase, at a local minimum above 650°C. The mineral

200   carbon (MINC) is the remaining fraction of the CO_2 and CO curves, calculated between 400-650°C in the pyrolysis phase and approximately between 650-850°C in the oxidation phase. To validate the usefulness of this discrimination, we also applied a loss-on-ignition (LOI) procedure to remove SOM and to identify the correct separation between soil organic carbon (SOC) and mineral carbon (MINC) (see Supplementary Material 1.5). SOC is calculated by summing the hydrocarbon signal (HC), CO, and CO_2 curves from both the pyrolysis and

205   oxidation phases. The HC peak, representing carbon in a reduced state, is used to calculate the hydrogen index (HI) of the SOC mg HC gr SOC^{-1}. The HC signal was also integrated in 4 parts representing different thermal stability regimes according to Sebag et al. (2016): A_1 (200-340°C), A_2 (340-400°C), A_3 (400-460°C), A_4 (460-650°C), which are used to calculate two indices: The R-index (RI) calculated as $(A_3+A_4)/A_{1-4}$ is indicative of the relatively thermal stable fraction of the HC, while the I-index ($\log_{10} [(A_1+A_2)/A_3]$) is indicative for the thermal

210   labile fraction of HC (Sebag et al., 2016). Similarly to the HI, the oxygen index (OI; mg CO_2 gr SOC^{-1}) represents the CO_2 released in the pyrolysis phase (200-400°C), corresponding to oxygen in the OM. The TpkS2 °C is the temperature at the maximum HC signal.

Calibration of sulfur signal in both the pyrolysis and combustion phases was done using pure organic S compound (Di-benzothiophene) and pure pyrite following Cohen Sadon et al. (2022). For real samples that

215   contain multiple S fractions, the organic and pyrite fractions are separated during the pyrolysis phase and can be distinguished by a local minimum at approximately 500°C (Cohen Sadon et al., 2022). However, during the oxidation phase, the residual organic and pyrite S are co-eluted at around 400°C, requiring an empirical relation to deconvolute (Cohen Sadon et al., 2022; Aboussou, 2018). Moreover, some of the pyritic S is retained during

pyrolysis at the presence of carbonates and is released at higher temperature (~700-900°C). Sulfate sulfur
220 measurement requires high temperatures and is released during combustion above 900-1000°C (Aboussou, 2018).
In this contribution the cutoff between retained S and sulfate signals was set manually to the local minimum
between them, at temperature of ~1000°C.

3.2 Soil incubation

Soil samples were oven-dried at 60°C overnight and then stored in the lab. Each profile consists of 6 samples,
225 each sample was gently grounded, if it contained large aggregates, and sieved to < 2 mm. From each sample, four
splits of 1.5 g portion of soil were weighed to 6 ml vessel, then distilled water was added to 60% of its water-
holding capacity. Water holding capacity was determined for degraded and pristine samples separately. This was
done by saturating 15 gr of soil with 50 ml distilled water and measuring the drained volume of water, using
Whatman 40 filter (8μm). All samples were preincubated for bacterial acclimation for five days at the designated
230 temperature. The experiments were aerobic and conducted in duplicates under two conditions: (1) for seven days
at 22°C, and (2) for two days at 33°C. During the incubations, gas samples were collected for CO_2 and O_2
concentration analyses. Samples were taken using glass flasks (~3.7 mL or ~13 mL, depending on incubation
duration) equipped with Louwer™ O-ring high-vacuum valves. Measurements were taken at halfway (t=1) and at
the end (t=2) of the experiment to validate a linear change in gas concentration during incubation. The O_2 and
235 CO_2 of the air samples were measured in the laboratory by a closed system (The "Hampadah"; Hilman and
Angert, 2016). The system is based on two analyzers: an infra-red gas analyzer (IRGA) for CO_2 measurement (LI
840A LI-COR; Lincoln, NE, USA) and a fuel-cell based analyzer (FC-10; Sable Systems International, Las
Vegas, NV, USA) for measuring O_2, and is fully automated. Each sample was incubated and measured in a
known volume, to derive the percentage and concentration of CO_2 and O_2. Fluxes rate, and reaction constant (k)
240 of CO_2 and O_2 were calculated for both 22°C and 33°C as shown in Equations 1 and 2, respectively. The apparent
respiratory quotient (ARQ), as shown in Equation 3, represents the ratio of CO_2 and O_2 fluxes (Angert et al.,
2015). This ratio provides information on the respiratory substrate stoichiometry as well as the underlying biotic
and abiotic processes (Hilman et al., 2022). Temperature sensitivity of organic matter decomposition, expressed
as Q_{10} (Eq. 4), is a metric for assessing the vulnerability of organic matter to temperature increases (Hilasvuori et
245 al., 2013). Q_{10} was calculated using the rate constant k, derived from respiration experiments conducted at 22°C
and 33°C, which represent the annual average soil temperature and its maximal summer temperature in Hula
valley, respectively.

$$(Eq. 1)\ Flux = \frac{CO_{2\ (t=2)}[\mu mol] - CO_{2\ ambient}[\mu mol]}{days * gr\ SOC}$$

250

$$(Eq. 2)\ k\ constant\ [yr^{-1}] = Flux * 12\ \frac{gr\ C}{mol} * \frac{1gr}{10^6\ \mu gr} * \frac{365\ days}{1\ yr}$$

$$(Eq. 3)\ ARQ = \frac{[CO_{2\ (t=2)}] - [CO_{2\ ambient}]}{[O_{2\ (t=2)}] - [O_{2\ ambient}]} \qquad (Eq. 4)\ Q_{10} = \frac{k(33°C)^{\frac{10}{33-22}}}{k(22°C)}$$

3.3 Statistical analysis

Statistical analyses were performed using JMP software (JMP®, JMP Pro 17, SAS Institute Inc., Cary, NC, USA). To determine difference between the peat column sections we used one-way analysis of variance (ANOVA) and Tukey-Kramer test. For unequal variances, we used a Welch's test and nonparametric comparisons using Steel-Dwass test. Significant differences were determined at $P < 0.05$.

260 The geochemical and respiration data were statistically analyzed based on three peat profile sections: drained, rewetted, and pristine, defined according to their respective historic and current WTL's (Table 1). The drained section included samples from depths of -30 cm to -100 cm, except for profile C, in which it extended to -180 cm. The rewetted section, available only in profiles E and F, ranged from -110 cm to -160 cm in profile E and -110 cm to -190 cm in profile F. The pristine section extended from -200 cm to -400 cm in profiles C, E, and F, while

265 in profiles A and D, it began at a depth of -150 cm. Samples containing more than 30% carbonate content were excluded from the statistical analysis to avoid incorporating lake mineral horizons, which were primarily found at the bottom of the profile.

3.4 Historical Data of SOM

270 Since its drainage in 1957, the 'deep peat' area of the Hula Valley (marked in Fig. 1) has been studied in numerous research projects, some of which have dealt specifically with SOM loss over time, such as the report by the Marish (1986) and Litaor et al., (2011). To assess the changes in peat soil organic matter (SOM) subjected to 66 years of drainage, we focused on the drained section identified in previous studies with multiple soil profiles (Schalinger et al., 1970; Yaari et al., 1971b; Marish, 1986, Litaor et al., 2003). We constrained our data

275 compilation to the boundaries of the 'deep peat' area to ensure consistency and avoid significant lithological variations, as well as the impact of soil fires, which mainly occurred south of this region. For depth selections, we

set the upper boundary at -30 cm to minimize the influence of agricultural practices such as soil tillage and root bias. To focus on the upper, drained peat, the lower boundary was established at -100 cm, which reflects the prevailing WTL in the region, given the spatial heterogeneity of the WTL. To convert the SOC results to SOM data, as reported by previous studies, we measured gravimetrically the SOM by removing SOM through combustion (using LOI_{400} procedure; Nelson and Sommers 1996) to a set of samples. We then correlated the SOM to SOC and applied a correction factor. Details of this correction are provided in the supplementary materials (1.5).

3.5   Fitted SOM Model

The modelling of organic matter loss through decomposition is a well-studied topic (Manzoni and Porporato, 2009), with various models proposed to represent these processes (Manzoni et al., 2012). Here we chose a model that comprises of two organic matter compartments (pools), as described by equation 5. These two pools are: 1) a labile SOM pool decomposing exponentially with reaction constant k and 2) a persistent SOM pool (SOM_P), which is inert, with no decomposition or formation. The SOM_i represents the initial value of the model, P denotes the fraction of persistent SOM out of SOM_i, t denotes time in years, and k serves as the reaction constant of SOM decomposition. The unknown parameters, k and SOM_P, are optimized to minimize the root mean square deviation (RMSD; Eq. 6), which quantifies the mean difference between model predictions and observed data. Where SOM_{data} represents field data from various studies, SOM_{model} denotes the simulated values, and n is the number of observations. The initial SOM (SOM_i) value is based on Ravikovitch 1948 work. Historical data and this current study (five data points, n=5) are used as the observed data (SOM_{data}) for RMSD calculation. The model simulates the long-term decline in organic matter following drainage from 1957 to 2023 (present study).

$$(Eq.5)\ SOM(t)_{[wt.\%]} = \left(SOM_i * (1 - P)\right) * e^{-kt} + (SOM_P)\ ,\qquad P = \frac{SOM_{P_{[wt.\%]}}}{SOM_{i_{[wt.\%]}}}$$

$$(Eq.6)\ RMSD = \sqrt{\frac{\sum_y^n (SOM_{data} - SOM_{model})^2}{n}}\ , n = 5$$

11

4   Results and Discussion

4.1   SOC oxidation and mineralization

Previous research on Hula peat has highlighted a decline in the SOM content within the drained section,
attributed to aerobic conditions (Marish, 1986; Litaor et al., 2011). Based on these findings, we hypothesize a
305 continued reduction in SOM content in the upper drained section and anticipate potential evidence of SOM
preservation in the rewetted section, which remained unexplored to date. Additionally, the pristine section, which
remained under anaerobic conditions, is expected to exhibit minimal variations in SOM content. Figure 2 shows
the measured SOC profiles wt.% from west to east, along with their corresponding WTL as detailed in Table 1.
Overall, SOC content in all profiles is lower in the drained and rewetted sections relative to the pristine section.
310 The profiles can be categorized into two main types: (1) profiles with similar post-drainage and post-rewetting
WTLs, resulting in only drained and pristine sections – profiles A, D and C, and (2) profiles with different
historical WTLs, creating a rewetted section between the drained and pristine sections – (profiles E and F). In
most profiles, there is a clear upward decline in SOC corresponding to the post-drainage WTL (light pink bars,
Fig. 2), indicating mineralization and SOC loss due to the lowering of the WTL. For instance, profiles A and C
315 (type 1) had relatively constant but different WTLs over 66 years of drainage. In both profiles, the depth in which
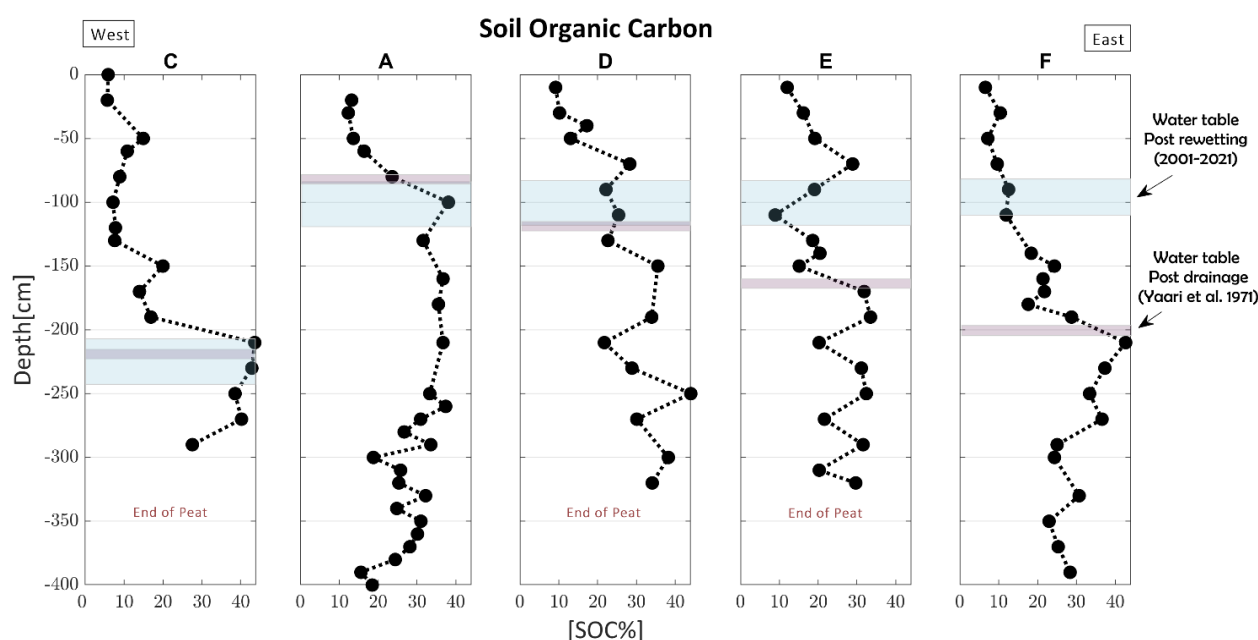SOC declines above it, aligns with the respective WTLs.

Figure 2: SOC profiles (from west to east) of peat cores with respective WTLs - post drainage (purple – after Yaari et al. 1971b)
and post rewetting (light blue – MIGAL Monitoring).

12

The trends in SOM content are further supported by additional organic geochemical data, such as the OI and RI indices. For example, a detailed composite plot of profile F (type 2) identifies three distinct sections (Fig. 3),
320   corresponding to drained, rewetted, and pristine conditions, separated by the historical WTL. Alongside the declining SOC trend, a negative relationship exists between SOC and both OI and RI, indicating that as peat degradation progresses, residual SOC becomes more oxidized, and the proportion of the thermally stable fraction increases. Similar coupling of the historical WTL and the trends of the organic geochemical proxies were found for the rest of the cores, and their composite plots are given in the Supplementary Material (1.4).

325   Sulfur species, obtained using the RE-7S, were distinguished as detailed in Supplementary Material 1.9. In the drained section, a decline in both organic sulfur and pyrite is evident, while sulfate accumulates, reflecting aerobic conditions (Fig. 3 and Supplementary Material 1.4). In contrast, the pristine and rewetted sections show low sulfate levels but high pyrite concentrations, with a maximum pyrite abundance in the rewetted section. Assuming that pyrite was fully oxidized in the rewetted section during its drainage period (37 years), this peak
330   likely represents a secondary pyrite formation through sulfate reduction under anaerobic conditions following rewetting. The peak in pyrite concentration beneath the recent WTL was observed in most profiles (supplementary material 1.4), suggesting a sulfur recycling mechanism in the drained and rewetted peat sections. Ultimately, pyrite serves as an indicator for both sulfate reduction in the sediment and recent WTL regimes. The corresponding respiration fluxes reveal two key points (Fig. 3 and supplementary material 1.4): (1) respiration
335   fluxes (normalized to SOC) in the drained and pristine sections are similar despite differences in SOC content and chemical properties (as indicated by OI and RI); and (2) respiration fluxes in the rewetted section are twice as high as in the other two sections. These findings are explored further in the next section. pH levels remain mostly neutral but drop to 5.9 in profile F and as low as 3.5 in other profiles. Litaor et al. (2011) also found pH levels of 5-3.8 at a depth of 50 cm in carbonate free horizons, which they interpreted to result from pyrite oxidation, and
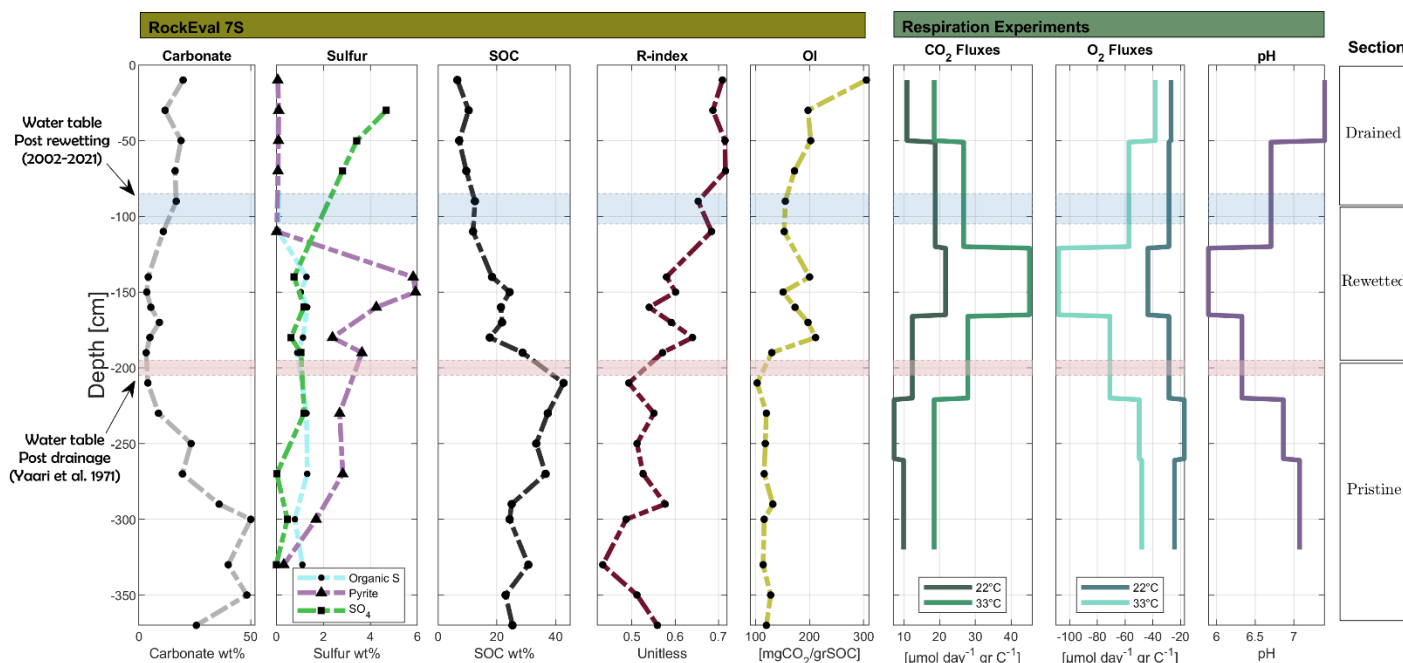340   nitrification.

Figure 3: Detailed composite plot for profile F, including the historic water table levels.

4.2 Average SOC characteristics of drained, rewetted and pristine peat

In the current section we present a statistical compilation of all the soil profiles data. The analyses are made for the predefined three peat column sections: drained, rewetted, and pristine. Figure 4 present the average thermal analysis indices for each section. Overview of the results and statistical tests for sections comparison are presented in supplementary Tables S1 and S2.

Significant difference ($p<0.05$) between all three section was found for SOC, TpkS2, RI, I-index and OI (one exception is that the drained OI values is not significantly different from the rewetted). The mean SOC values for the drained, rewetted, and pristine sections are 13 ± 1, 20 ± 2 and 35 ± 1 wt.%, respectively. Thus, it is evident that 66 years of drainage have led to extensive degradation, reducing SOC to approximately one-third of its original pristine value, without considering compaction processes. The rewetted section shows higher SOC content than the drained section, suggesting that degradation ceased or decreased following rewetting. The OI shows a reverse pattern to the SOC, with a gradual decrease in its mean value from the drained to the rewetted and pristine sections (195 ± 7, 160 ± 11 and 100 ± 7 mg CO_2 gr SOC^{-1}, respectively). This can indicate a partial oxidation of the SOM due to drainage and a slowdown in oxidation due to rewetting. This observation is further supported by

14

other SOM thermal indices (Fig.4; correlation in supplementary Fig.S6). Mean TpkS2 values for the drained, rewetted, and pristine sections are 460 ±5, 431 ±7 and 378 ±5 °C, showing the increase of HC peak temperature along with degradation and SOC decline. The mean RI values for the drained, rewetted, and pristine sections are 0.67 ±0.01, 0.59 ±0.02, and 0.49 ±0.01, respectively, while the mean I-index are -0.03 ±0.01, 0.1 ±0.02 and 0.26
360 ±0.01, respectively (Table S1). While the RI and I-index values of the pristine section represent organic soil, those of the rewetted and drained sections fall into the range typical for organic-mineral and mineral soil horizons (Sebag et al., 2016). The RI values of the drained and pristine peatlands further align with the findings by Brown et al. (2023), who reported higher RI values for disturbed peat sites compared to pristine peat sites, all measured from the top 50 cm peat layer (duration since drainage was not specified).

365 Together, these results demonstrate that with decomposition the residual SOM becomes more oxidized and contains a lower proportion of thermally labile compounds. The increase in thermal stability could be due to a relative increase of litter recalcitrant material (Könönen et al., 2016; Barré et al., 2016), that the residual SOM is minerals associated (Saenger et al., 2015), or both. Moreover, the rewetted section exhibits a higher degree of SOM preservation compared to the drained section, highlighting the impact of rewetting on reducing degradation.
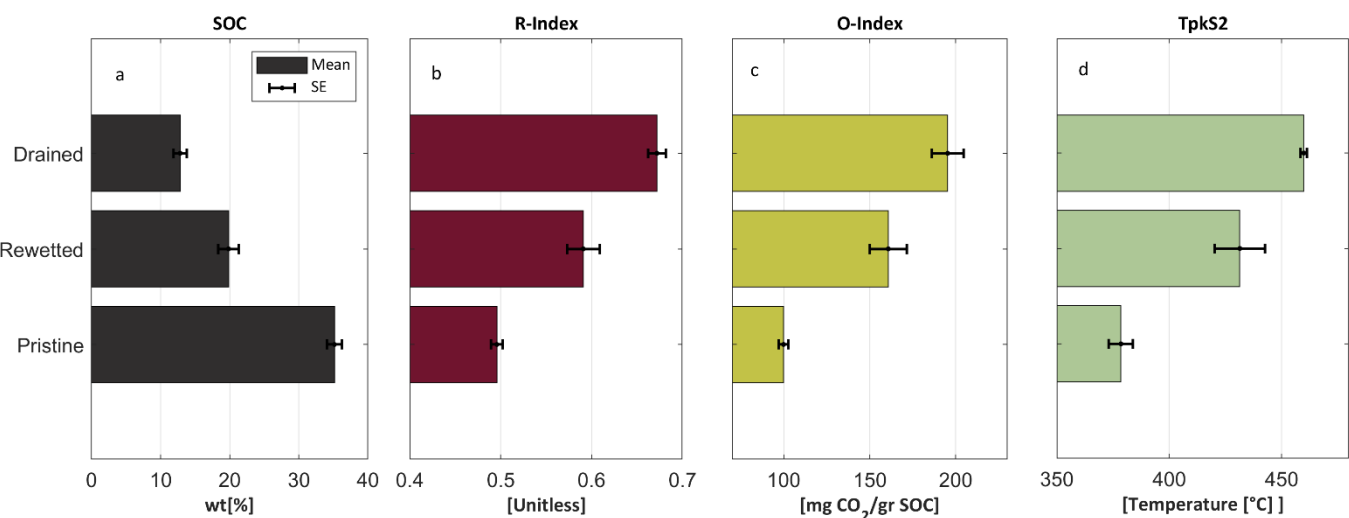

Figure 4: Rock Eval analysis results - mean value and standard error of all the profiles from three sections[cm]: drained [30-100] (n=25), rewetted [110-170] (n=10) and pristine [200-400] (n=26). (a) SOC content, (b) R-index, (c) Oxygen index and (d) HC peak temperature - TpkS2.
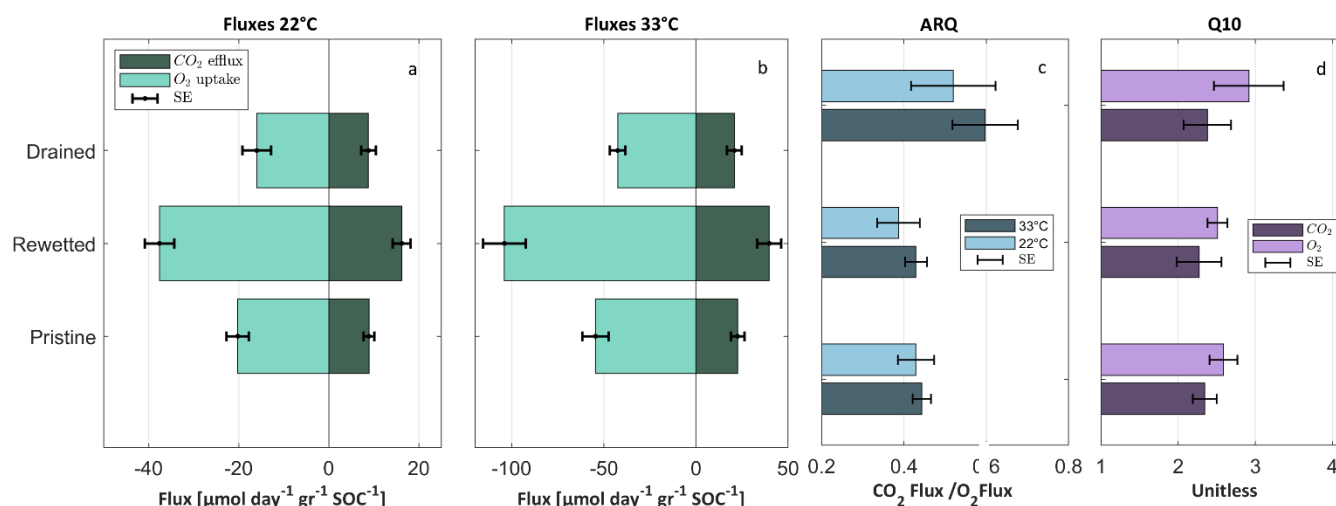
370

Figure 5: Respiration experiment results - mean value and standard error of all the profiles from three sections[cm]: drained [30-100] (n=8), rewetted [110-170] (n=4) and pristine [200-400] (n=12). (a) CO_2 and O_2 fluxes at 22°C experiments. (b) CO_2 and O_2 fluxes at 33°C experiments. (c) ARQ -CO_2 fluxes divided by O_2 fluxes derived from 22°C and 33°C experiments. (d) Q10- derived from CO_2 and O_2 k constant.

The experimental respiration results were also statistically analyzed in each of the defined sections for all the profiles collectively. Figure 5 displays the mean CO_2 and O_2 fluxes per gram of SOC at 22°C and 33°C, and their

375   derivatives indices – ARQ and Q_{10}. Mean fluxes of CO_2 of the drained, rewetted, and pristine sections at 22°C were 9 ±2,16 ±2 and 9 ±1 µmol CO_2 gr SOC^{-1} day^{-1}, respectively (Fig. 5a), showing a similar flux for the drained and pristine sections, and approximately a double flux in the rewetted section. This pattern is also evident for the O_2 fluxes at 22°C (-16 ±3, -37 ±4 and -20 ±2 µmol O_2 gr SOC^{-1} day^{-1}) for the drained, rewetted and pristine sections, respectively; Fig. 5a). The same pattern is evident in the 33°C experiments in both CO_2 and O_2 (Fig.

380   5b), reinforcing the reliability of this finding. We found similar fluxes in the drained and pristine sections despite the distinctly their different SOC, RI and OI values (Fig. 4). A similar observation was made by Bader et al. (2017), which also found that the degraded peat horizon in cold temperate sites exhibited similar flux per SOC as deeper, less disturbed peat. Moreover, in our study, the rewetted section which has intermediate SOC, RI and OI values (compared with the pristine and drained sections), had the highest respiration fluxes. These results indicate

385   that SOC content and RE-7S proxies (RI, OI, and I-index) do not directly reflect SOM bioavailability for short-term bacterial respiration.

The first order reaction constant k (Eq. 2) was calculated for aerobic SOC decomposition at 22°C, resulting in - 0.037, -0.087 and -0.033 yr^{-1}, for the drained, rewetted and pristine sections, respectively. Temperature sensitivity, as indicated by the mean Q_{10} values, for O_2 fluxes was 2.9 ±0.4 for the drained section and 2.5 ± 0.4

390   for the pristine and rewetted sections, with no significant difference between the sections. Mean Q_{10} values from CO_2 of across all sections were relativity similar (2.3 ±0.3), with no statistically significant difference (Table S2). Bader et al. (2017) found that the mean Q_{10} (derived from CO_2 flux) for drained peatlands in cold temperate sites was 2.5 ±0.1, which resembles our findings despite the different climate.

The ARQ results also show no significant difference between the sections, with mean values at 22°C of 0.6 ±0.05

395   ,0.43 ±0.07 and 0.45 ±0.04, for the drained, rewetted and pristine sections, respectively. In aerobic conditions the expected ARQ value can be indicative of the oxidation state of the decomposed organic carbon compounds (Hilman et al., 2022). Values of ARQ of 1.0 are attribute to sugars which are more labile, while lower values are attribute to compounds such as lipids (0.73) or proteins (0.77), which can derive from necromass and more recalcitrant material (Masiello et al., 2008; Hicks Pries et al., 2020). However, the pristine and rewetted ARQ

400   results show lower values that are not attributed to any compound and thus may indicate oxygen consumption by partial oxidation of SOM or oxidation of reduced chemical species such as Fe^{2+} or sulfides (Markel., et al 1998).

4.3 Long-term SOM decomposition in the Hula's drained peat

The Hula peat exhibits lithological variations both spatially and with depth, resulting from the natural habitat's

405   dependence on varying water regimes and plant diversity. Additionally, as mentioned above, a decline in SOM of Hula's peat since its drainage was reported (Marish, 1986; Litaor et al., 2011). Here, we evaluate long-term (7 decades) decomposition of peat in the field, by compiling literature data focusing on the top drained section. To this end, studies that included comprehensive data of spatial distribution and sampling depths together with evaluations of SOM of the drained section (30-100 cm) were compiled and analyzed. The SOC data from this

410   study were converted to SOM using correlations factors for the Hula peat soils determined here as 1.6 for drained samples and 1.8 for pristine samples (Supplementary Fig. S3). The full data set is summarized in Table 2 and illustrated in Fig. 6, alongside our SOM analysis.

During the 66 years of drainage the mean SOM content of the top layer significantly decreased from 68±4% to 21±2% (Fig. 6). This decline was continuous, following an exponential decay pattern, with the most substantial

415   loss of organic matter occurring during the first three decades, after which the rate of SOM decomposition slowed. Notably, the initial SOM value reported by Ravikovitch in 1948 aligns closely with the SOM of the

pristine section in our study (2023), supporting the concept of preservation under saturated conditions (Fig. 6). Additionally, the SOM value in the rewetted section also conforms to this timeline, suggesting that it has remained mostly unchanged since 1994. These agreements are illustrated by the grey arrows in Fig. 6.

Table 2. Changes in soil organic matter content in the Hula deep peat area since the drainage.

Year	Study	Mean SOM% ± SE	n	Spatial n	Depth [cm]	LOI Method
1948[a]	Ravikovitch 1948	68 ± 4	4	3	0-100	Not reported
1970	Schalinger et al., 1970	48 ± 2	30	10	25-100	Not reported
1971	Yaari et al., 1971	47 ± 3	10	9	40-110	Method 1
1986	Marish, 1986	33 ± 2	9	4	40-100	Not reported
2000	Litaor et al., 2003	31 ± 4	27	27	50	Method 2
2023	This Study	21 ± 2	20	5	30-100	Method 3
2023	This Study	33± 2	8	2	110-170	Method 3
2023	This Study	64 ± 2	23	5	200-400	Method 3

Method 1: LOI at 850°C and carbonate correction following acid digestion. **Method 2:** Acid digestion and LOI at 850°C.
Method 3: This study - SOC analysis with RE-7S and LOI at 400°C conversion (Supplementary 1.5).
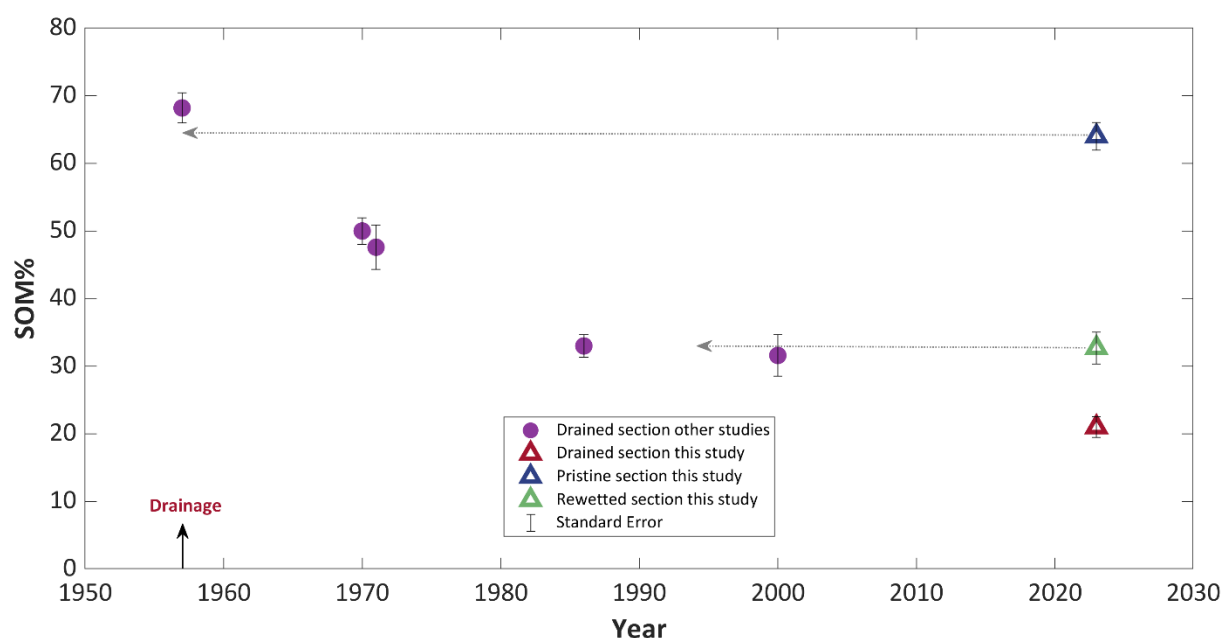

Figure 6: Mean soil organic matter (SOM) content of Hula peat since the drainage, based on data from this study (triangles) and historical studies (Purple circles). All from depths of 30-100 cm.

420

4.4 The two-pool SOM model

The decay pattern in Fig. 6 shows an exponential decline, a behavior similar to long-term Bare Fallow experiments of mineral soils (Barre et al., 2010). To better understand the long-term decomposition process of Hula's peat, we explored the observed SOM data with a model. A simple one-box model proved inadequate for

425 capturing the decomposition process of SOM in mineral soils (Barré et al., 2010; Manzoni et al., 2012; Clivot et al., 2019). The long-term data of Manzoni et al. (2012), based on the Rothamsted Bare Fallow experiment, serves as a good analog to Hula's peat SOM for two reasons: (1) it involves decomposition without significant additional organic matter inputs, and (2) it follows an exponential decomposition pattern over time. Manzoni et al. (2012) suggest that a two-pool model effectively captures long-term soil respiration dynamics, making further

430 complexity unnecessary. Comparable models were used by Barré et al. (2010) and Cécillon et al. (2021), in which one pool undergoes exponential decay while the other remains stable. Other models account for plant input flux (e.g., the AMG model; Clivot et al., 2019) and leaching of dissolved organic carbon as a pathway for SOM decomposition (e.g., Page et al., 2016, Rixen et al., 2016). Here we assume that plant input to the deep peat (i.e., below 30 cm) is negligible and focus on total SOM loss rather than specific pathways (i.e., respiration vs. DOC

435 leaching). In addition, although seasonal soil moisture and temperature variations influence SOM decomposition rates, their effects were not addressed explicitly in this analysis. Ultimately, we adopted a two-pool model, where a persistent pool of SOM is initially present and assumed to have a negligible decay rate, while a labile-intermediate pool is consumed with a single reaction constant (Eq. 5).

4.5 The SOM Model results

440 As discussed above the drained and pristine sections of Hula peat have similar respiration fluxes per SOC unit, both for the CO_2 efflux and the O_2 influx (Fig.5). Similarly, Bader et al. (2017) also found, in their study of peat in temperate-cold climate, that respiration rates per SOC unit in drained and undisturbed peat are comparable. Thus, we suggest that both the pristine and drained peat sections can be characterized by the same reaction constant (see Eq. 5), despite their different organic characteristics. Practically, this similarity allows for a fixed

445 reaction constant (k) to be applied to the labile SOM pool throughout the entire model duration. Also, the similarity of the present-day pristine SOM value to those reported by Ravikovitch 1948 (i.e., pre-drainage) allows us to assume a value of 68 ± 4 wt.% for the initial SOM_i.

Hence, our two-pool model includes two unknown variables: SOM_P and k. With these two degrees of freedom, the model yields a range of possible solutions. The model was run with multiple SOM_P and k values, and the
450   RMSD was calculated for each run (Eq. 6). Plotting SOM_P versus k and RMSD for all the runs (Fig. S1) reveals that the two unknown variables are related and identifies a single local minimum for the solutions RMSD. In Fig. 7, we illustrate the model results as an envelope of those possible solutions (grey area). This envelope represents model solutions with the lowest RMSD values, defined by a maximum RMSD of 2.2 wt.% of SOM, which ensures that all observed data fit within their standard error. The resulting model envelope ranges for k and SOM_P
455   are -0.03 to -0.042 yr^{-1} and 13–21 wt.%, respectively. To further constrain our model results, we incorporated the reaction constant (k) measured by the CO_2 fluxes in the short-term respiration experiments at 22°C (which is the mean annual temperature) to the model (Fig. 5a). This reduces the model solution to a single degree of freedom, enabling a direct comparison with the two degrees of freedom model solution. Since the experimental k constant is calculated for the entire SOC content, it must be corrected if $SOM_p>0$ according to the labile SOM k corrected
460    $=k$ experimental $/(1-P)$]. Assuming SOM_P of 17 wt.% (the median result of the two degrees of freedom model run), the experimental $k_{corrected}$ constant is -0.044 ± 0.005 yr^{-1} (Fig. 7, green shade). Additionally, we run the model assuming no SOM_p ($SOM_p=0$) and as a result the experimental respiration k constant had no correction factor (k=-0.033 ± 0.004 yr^{-1}; Fig. 7, blue line).

As Fig. 7 shows, using the experiment k as an input, and assuming that there is no stable fraction of SOM
465   ($SOM_p=0$), results in a predicted decomposition (blue line) which is much faster compared with the field data. This model run predicts a SOM content in 2023 of approximately 8%, which is inconsistent with the observed value of 21%. In contrast, the model run which used the experimental k and a SOM_p value of 17% (green envelope), effectively explains the field data and aligns closely with the RMSD envelope of the two degrees of freedom run (grey envelope). Therefore, the short-term respiration experiments can be used to bridge the gap
470   with long-term (70-years) process of peat degradation, at least at this site. In summary, we suggest that peat degradation is a process lasting several decades under a warm climate, during which a fraction of persistent organic matter remains in the soil, even after long-term degradation given the prevailing land-use practices.
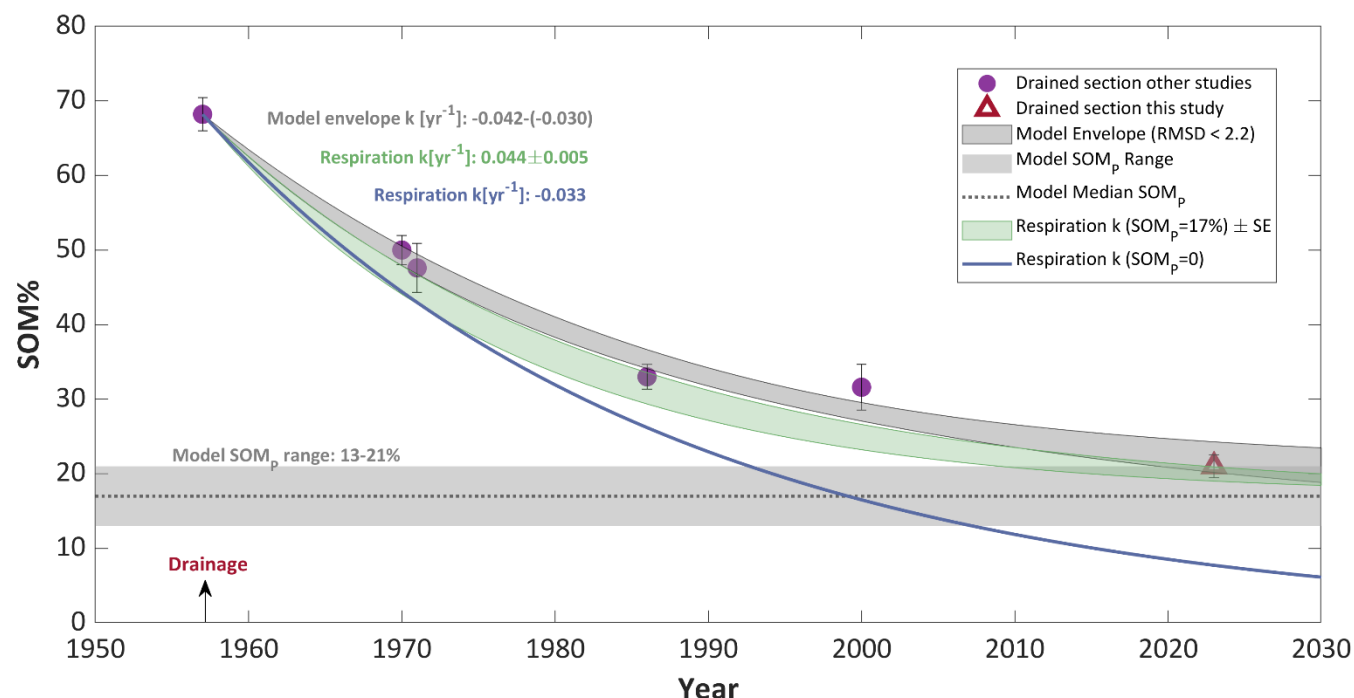
Figure 7: Mean soil organic matter content of the upper 1 meter of Hula peat since drainage in 1957, represented by markers. The fitted model result is shown by the grey envelope of possible solutions with RMSD lower than 2.2% SOM. The horizontal grey area and dashed line represent the persistent SOM pool range and median, respectively, predicted by the model. The experimental respiration decay result is represented by the green area (width is indicating the standard error), assuming 17% SOM_P. The blue line shows the result of the experimental k with zero SOM_P.

4.6   The model limitations

475   It is important to note some limitations: (1) our analysis assumes the drained section has not been significantly affected by the partial rewetting initiated in 1994. While this section technically remains drained after the rewetting project, the increase in water content could influence soil respiration and potentially alter decomposition rates, either enhancing or reducing them. (2) The respiration experiment might overestimate the actual rate since it is measured in optimal water holding capacity (60%), which does not typically occur in natural

480   settings. We suggest that this might be the reason for the experimental k plot to project somewhat more intense decomposition compared to the observed data (Fig. 7, green shade). (3) Another potential limitation is the possibility of enhanced decomposition in the drained section due to the priming effect caused by root exudates from crops (Fontaine et al., 2004). However, Linkosalmi et al. (2012) found no evidence of a priming effect in

their study of drained peatlands, suggesting that the introduction of labile carbon substrates, such as root
485 exudates, did not significantly accelerate the decomposition of older, more persistent organic matter. (4) It is
acknowledged that additional SOM inputs and outputs that are not accounted for in the model may contribute to
the overall trend. These may be root carbon contributions or DOC leaching for example. While the model, which
is based on observed data, effectively captures the overall SOM losses and gains, this remains a limitation when
directly comparing it to respiration fluxes. Nevertheless, as pointed out above, we find the model in its current
490 form - both satisfactory and informative.

4.7 Persistent SOM in the Hula peat

While our model analysis suggests the presence of original persistent SOM and further confirms it by including
the short-term experiments' decomposition rate constant, direct evidence for persistent SOM is still lacking.
Recent studies have attempted to quantify persistent SOC using Rock-Eval analysis (Saenger et al., 2015;
495 Cécillon et al., 2021). Here, we discuss this knowledge regarding SOC persistence in relation to our findings.
Such persistent SOM could have been an original fraction of the peat or formed during the oxidation process or
resulted from a combination of both. Furthermore, the mechanism behind its persistence (e.g., mineral association
or other processes) in drained peat remains unknown.

In addition to our SOM model, the correlation between mean SOC and RI values across sections highlights the
500 increase in thermal stability of the drained section compared to the pristine section. Figure 8a presents pyrograms
of the Rock-Eval HC signal generated during the pyrolysis ramping. It shows that pristine samples (blue curves)
exhibit two dominant HC peaks, corresponding to thermally labile and stable fractions (Sebag et al., 2016). In
drained samples, these peaks persist but are diminished, with the high-temperature peak less reduced. This
suggests that during drainage, as bacterial activity accelerates organic matter decomposition, the thermally labile
505 fraction (up to 400°C) is preferentially consumed, leaving behind residual thermally stable SOC, contributing to
higher RI values in drained samples.

The mechanism and evaluation of persistent SOC has been widely studied and debated (Cécillon et al., 2021).
Barré et al. (2016), Gregorich et al. (2015), and Saenger et al. (2015) demonstrate that while persistent SOM has
diverse chemical compositions, it generally exhibits low energy content and hydrogen depletion, making it more
510 refractory at high temperatures. This aligns with our findings (Fig. 8). Saenger et al. (2015) proposed a thermal
fractionation of SOC using RE analysis, identifying three SOC pools based on the pyrolysis HC curve: labile,
particulate, and mineral-associated SOC - a classification widely accepted in soil science.
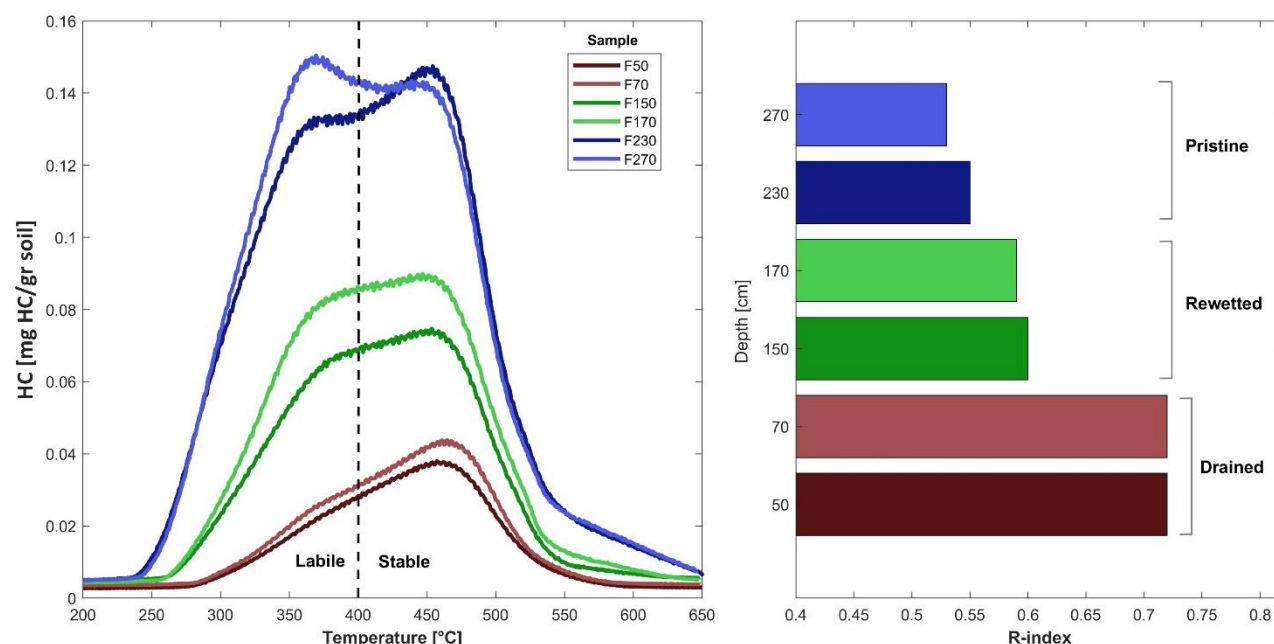
22

Figure 8: (a) FID signal curves of hydrocarbons for pristine, rewetted, and drained samples from profile F, with colour scheme by section type and depth. The dashed line separates labile and stable hydrocarbons, following the method used for RI (Sebag et al., 2016). (b) RI values for the same samples, using the same colour scheme.

Our thermal analysis partially aligns with these findings. The stable SOC HC peak (above 450°C), attributed by Saenger et al. (2015) to mineral-associated SOC, appears in all sections. In pristine samples, it is as high as the

515   labile SOC peak. However, mineral association with SOC is expected to be very low in pristine peat samples (Mirabito and Chambers, 2023). This demonstrates that attributing HC peaks to particulate and mineral-associated SOC presents a challenge in Hula's peat.

A new approach to estimating persistent SOC in soils using Rock-Eval was proposed by Cécillon et al. (2021)

520   through the PARTYsoc model (v2.0). The results indicate that, unlike the thermal indices we used above, the predicted stable SOM by the PARTYsoc model showed only a weak negative correlation with SOC content ($R^2 = 0.25$; supplementary material 1.6). The model estimates of the stable fraction was multiplied by the SOC content, yielding a mean persistent SOC of 13.2 ± 0.8 wt.% in the pristine section and 6.1 ± 0.5 wt.% in the drained section. However, persistent SOC is not expected to decline so fast during 66 years of peat decomposition since it

525   is defined as resilient for more than a century (Cécillon et al., 2021), suggesting a discrepancy in these results.

Our findings show that the estimation of the PARTYsoc v2.0 model or pool separation by Saenger et al. (2015) is inadequate for the Hula's peat. However, while RI does not deliberate quantification of persistent SOC, it could serve as a practical and effective tool for analyzing and comparing degraded peat SOC, both in research contexts and for peatland management.

530 ## 4.8   Estimation of annual CO_2 emissions

Respiration models and global annual emission estimates typically incorporate factors such as peat SOM content, bulk density (BD), and WTL. However, these models often neglect the critical factor of time since drainage, which significantly influences emission rates (Hooijer et al., 2010; Tubiello et al., 2016). To emphasize the impact of drainage duration on carbon fluxes, we compared respiration data from pristine and drained sections of

535 the Hula, representing the onset of drainage and nearly 70 years of degradation, respectively. The average annual carbon emissions flux from the pristine and drained peat sections of the Hula at 22°C, derived from the short-terms experiments (Flux per gr soil; Eq.1), are 12 ± 1 and 4.7 ± 0.9 mg C gr soil^{-1} yr^{-1}, respectively. Additionally, the average annual carbon loss rates derived from the observation-based long-term model (Fig. 7, grey area), calculated as (SOC$_{intial}$ - SOC $_{(10yr)}$)/10, are 9 ± 1 and 1.4 ± 0.2 mg C gr soil^{-1} yr^{-1} for the 1st and current 7th

540 decades, respectively. These two independent methods demonstrate the drastic difference in CO_2 fluxes between early and advanced stages of peat degradation. The comparison between these fluxes is presented in Fig. 9.
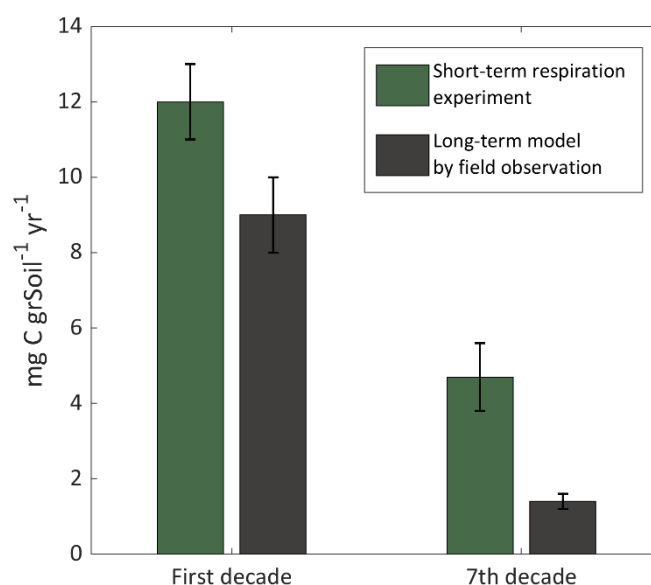

Figure 9: Average annual fluxes of CO_2 from peat soil, derived from short-term experiment (green) and long-term field model (black).

24

The IPCC and global models estimate CO_2 emissions from drained tropical peatlands at 73 ± 14 tons CO_2 ha^{-1} yr^{-1} (Hiraishi et al., 2013; Tubiello et al., 2016). To compare our results with flux rates from warm climate regions, we calculated a theoretical CO_2 emission value for a 100 cm drained peat column, using our experimental fluxes at 22°C (annual average) and bulk density of 0.22 g cm^{-3} (Dansberg et al., 1973). The estimated CO_2 emission is 94 ± 10 tons CO_2 ha^{-1} yr^{-1}, reflecting emissions during the initial decades after drainage, and is comparable with the IPCC estimates. After 66 years of degradation, assuming 70% soil shrinkage (Yaari et al., 1971b) and an increase in BD to 0.55 g cm^{-3} (Orlov-Levin and Meron, 2005), the current estimated CO_2 emission from the drained section is 28 ± 5 tons CO_2 ha^{-1} yr^{-1}.

5   Conclusions

Our observations show that active land management that includes partial rewetting of once drained peat column significantly mitigates CO_2 emissions and organic carbon loss, demonstrating its effectiveness even after prolonged drainage in a warm climate. The respiration results highlight the vulnerability of the rewetted peat horizon to re-exposure to air, showing the potential of enhanced fluxes, twice as high relative to the drained and pristine sections (per SOC). We also found a peak in pyrite concentration beneath the recent WTL, and sulfate accumulation in the drained section, which indicates sulfur recycling and anaerobic conditions. Short-term respiration experiments reveal that the drained and pristine sections share similar first-order reaction rates (k) for SOM decomposition, and that these experiments successfully describe the observed long-term SOM decomposition in the warm-climate Hula's peat. Model analysis, supported by those experimental results, indicate that approximately 13–21 wt.% of the ~68 wt.% initial SOM persists as a stable fraction in the drained peat, emphasizing the role of the persistent organic pool in stabilizing carbon stocks. However, the mechanism of persistence SOM formation in degraded peatlands requires further investigation. The use of a thermal analysis (Rock-Eval) to characterize the OM properties, coupled with short-term aerobic respiration experiments is shown here to be useful in bridging the gap to the field scale, to the modelling of long-term decomposition of peatlands, and to estimating their CO_2 emissions. The timeline of drained peat SOM decomposition shows that the first few decades are crucial, as SOM declines rapidly, resulting in high CO_2 emissions. Future peatland restoration projects, especially in warm climates, can use this site as an analogue to make more informed decisions for the priorities for sites rewetting.

570 **6 Acknowledgments**

We would like to express our gratitude to the Hula Valley Monitoring Program, operated by the MIGAL Institute, Tel-Hai College, and the Israel Water Survey, for their valuable collaboration and the availability of their data online. We also thank to Michael Litaor and Oren Reichman for providing access to their field data. We would like to acknowledge Tal Weiner, Roee Katzir and Itay Eyal for their assistance in our field work.

575 **7 Code availability**

The code for the peat SOM Model can be accessed in this DOI link: https://doi.org/10.5281/zenodo.15635973 .

8 Data availability

Data of Rock-Eval 7 analysis and respiration experiments can be accessed in this DOI link:
https://doi.org/10.5281/zenodo.15635973 .

580

9 Author contribution

The Investigation was done by GS. AA, RG, and YR conceptualized the research, were in charge on the methodology, and supervised GS. GS wrote the original draft , and AA, RG and Y reviewed and edited it.

10 Competing interests

585 The authors declare that they have no conflict of interest.

11 Sample availability

Samples are stored in the Geological survey of Israel and can be accessed if needed, please reach the author for more information.

12 Disclaimer

590 OpenAI was used solely to improve the grammar and phrasing of the text. The authors declare that no other artificial intelligence or machine learning tools were employed in this study.

13 References

Aboussou, A. New Rock-Eval method for Pyritic and Organic Sulphur quantification: Application to study Organic Matter preservation in Jurassic sediments (Doctoral dissertation, Sorbonne Université), 595 https://doi.org/10.13140/RG.2.2.27845.68324, 2018.

Angert, A., Yakir, D., Rodeghiero, M., Preisler, Y., Davidson, E. A., and Weiner, T. Using O2 to study the relationships between soil CO2 efflux and soil respiration. Biogeosciences, 12(7), 2089., https://doi.org/10.5194/bg-12-2089-2015, 2015.

Bader, C., Müller, M., Schulin, R., and Leifeld, J. Peat decomposability in managed organic soils in relation to land use, organic matter composition and temperature Copernicus GmbH., https://doi.org/10.5194/bg-15-703-2018, 2018.

600 Barré, P., Eglin, T., Christensen, B. T., Ciais, P., Houot, S., Kätterer, T., . . . Chenu, C. Quantifying and isolating stable soil organic carbon using long-term bare fallow experiments. Biogeosciences, 7(11), 3839., https://doi.org/10.5194/bg-7-3839-2010, 2010.

Barré, P., Plante, A. F., Cécillon, L., Lutfalla, S., Baudin, F., Bernard, S., . . . Chenu, C. The energetic and chemical signatures of persistent soil organic matter. Biogeochemistry, 130(1-2), 1., https://doi.org/10.1007/s10533-016-0246-0, 2016.

605 Behar, F., Beaumont, V. D. E. B., and Penteado, H. D. B. Rock-Eval 6 technology: performances and developments. Oil and Gas Science and Technology, 56(2), 111-134., https://doi.org/10.2516/ogst:2001013, 2001.

Bein, A. Hula valley report by the Geological Survey of Israel. (in Hebrew)., 1967.

Bein, A. Early evolution and transformation of organic matter in the active continental Jordan Rift Valley. Organic geochemistry, 10(4-6), 751-757., https://doi.org/10.1016/S0146-6380(86)80012-2, 1986.

610 Bein, A., & Horowitz, A. Papyrus-A historic newcomer to the Hula Valley Israel?. *Review of palaeobotany and palynology*, *47*(1-2), 89-95. https://doi.org/10.1016/0034-6667(86)90007-2, 1986.

Blume, H. P., Brümmer, G. W., Fleige, H., Horn, R., Kandeler, E., Kögel-Knabner, I., ... and Wilke, B. M. Soil organic matter. Scheffer/Schachtschabel Soil Science, 55-86., https://doi.org/10.1007/978-3-662-49880-4_3, 2016.

Bond-lamberty, B., Ballantyne, A., Berryman, E., Fluet-chouinard, E., Jian, J., Morris, K. A., . . . Vargas, R. Twenty years of 615 progress, challenges, and opportunities in measuring and understanding soil respiration American Geophysical Union (AGU)., https://doi.org/10.1029/2023jg007637, 2024.

Cécillon, L., Baudin, F., Chenu, C., Christensen, B. T., Franko, U., Houot, S., ... and Barré, P. Partitioning soil organic carbon into its centennially stable and active fractions with machine-learning models based on Rock-Eval® thermal analysis (PARTY SOC v2. 0 and PARTY SOC v2. 0 EU). Geoscientific Model Development, 14(6), 3879-3898., 620 https://doi.org/10.5194/gmd-14-3879-2021, 2021.

Chenu, C., and Cosentino, D. Microbial regulation of soil structural dynamics. In The architecture and biology of soils: life in inner space (pp. 37-70). Wallingford UK: CABI., https://doi.org/10.1079/9781845935320.0037, 2011.

Clivot, H., Mouny, J. C., Duparque, A., Dinh, J. L., Denoroy, P., Houot, S., ... and Mary, B. Modeling soil organic carbon evolution in long-term arable experiments with AMG model. Environmental modelling and software, 118, 99-113., https://doi.org/10.1016/j.envsoft.2019.04.004, 2019.

Clymo, R. S., Turunen, J., and Tolonen, K. Carbon accumulation in peatland. Oikos, 368-388., https://doi.org/10.2307/3547086, 1998.

Cohen-Sadon, H., Amrani, A., Feinstein, S., and Rosenberg, Y. O. A new empirical approach for rapid quantification of organic and pyritic sulfur in sedimentary rocks using the Rock-Eval 7S. Organic Geochemistry, 166, 104350., https://doi.org/10.1016/j.orggeochem.2022.104350, 2022.

Convention on Wetlands. Global guidelines for peatland rewetting and restoration. Ramsar technical report no. 11. Gland, Switzerland: Secretariat of the Convention on Wetlands., 2021.

Fontaine, S., Bardoux, G., Abbadie, L., and Mariotti, A. Carbon input to soil may decrease soil carbon content. Ecology letters, 7(4), 314-320., https://doi.org/10.1111/j.1461-0248.2004.00579.x, 2004.

Freeman, C., Ostle, N. J., Fenner, N. and Kang, H. A regulatory role for phenol oxidase during decomposition in peatlands. Soil Biol. Biochem. 36, 1663--1667., https://doi.org/10.1016/j.soilbio.2004.07.012, 2004.

Hambright, K. D., and Zohary, T. Lakes Hula and Agmon: destruction and creation of wetland ecosystems in northern Israel. Wetlands Ecology and Management, 6, 83-89., https://doi.org/10.1023/A:1008494705994, 1998.

Hicks Pries, C., Angert, A., Castanha, C., Hilman, B., and Torn, M. S. Using respiration quotients to track changing sources of soil respiration seasonally and with experimental warming. Biogeosciences, 17(12), 3045., https://doi.org/10.5194/bg-17-3045-2020, 2020.

Hilasvuori, E., Akujärvi, A., Fritze, H., Karhu, K., Laiho, R., Mäkiranta, P., . . . Liski, J. Temperature sensitivity of decomposition in a peat profile. Soil Biology and Biochemistry, 67, 47., https://doi.org/10.1016/j.soilbio.2013.08.009, 2013.

Hilman, B., and Angert, A. Measuring the ratio of CO_2efflux to O_2influx in tree stem respiration. Tree Physiology, https://doi.org/10.1093/treephys/tpw057, 2016.

Hilman, B., Weiner, T., Haran, T., Masiello, C. A., Gao, X., and Angert, A. The apparent respiratory quotient of soils and tree stems and the processes that control it American Geophysical Union (AGU)., https://doi.org/10.1029/2021jg006676, 2022.

Hiraishi, T., Krug, T., Tanabe, K., Srivastava, N., Baasansuren, J., Fukuda, M., and Troxler, T. G. 2013 supplement to the 2006 IPCC guidelines for national greenhouse gas inventories: Wetlands. IPCC, Switzerland., 2014.

Hooijer, A., Page, S., Canadell, J. G., Silvius, M., Kwadijk, J., Wösten, H., and Jauhiainen, J. Current and future CO_2 emissions from drained peatlands in southeast Asia. Biogeosciences, 7(5), 1505--1514., https://doi.org/10.5194/bg-7-1505-2010, 2010.

Orlov-Levin, V., and Meron, M. Soil salinization in Hula Valley crops -- Report (Report, in Hebrew). Israel Ministry of Agriculture., 2005.

Joosten, H., and Clarke, D. Wise use of mires and peatlands. International mire conservation group and international peat society, 304., 2002.

Kleber, M., Eusterhues, K., Keiluweit, M., Mikutta, C., Mikutta, R., and Nico, P. S. Chapter One---Mineral--Organic associations: Formation, properties, and relevance in soil environments. Advances in Agronomy, 130, 1., https://doi.org/10.1016/bs.agron.2014.10.005, 2015.

660

Kleinen, T., Brovkin, V., and Schuldt, R. J. A dynamic model of wetland extent and peat accumulation: results for the Holocene. Biogeosciences, 9(1), 235-248., https://doi.org/10.5194/bg-9-235-2012, 2012.

Könönen, M., Jauhiainen, J. R., Laiho, R. P., Spetz, P. K., Kusin, K. S., Limin, S. H., and Vasander, H. Land use increases the recalcitrance of tropical peat. Wetlands Ecology and Management, 24(6), 717., https://doi.org/10.1007/s11273-016-9498-7, 2016.

665

Leifeld, J., and Menichetti, L. The underappreciated potential of peatlands in global climate change mitigation strategies. Nature Communications, 9(1), https://doi.org/10.1038/s41467-018-03406-6, 2018.

Leifeld, J., Steffens, M., and Galego-sala, A. Sensitivity of peatland carbon loss to organic matter quality American Geophysical Union (AGU)., https://doi.org/10.1029/2012gl051856, 2012.

670 Liang, C., Schimel, J. P., and Jastrow, J. D. The importance of anabolism in microbial control over soil carbon storage. Nature Microbiology, 2(8), https://doi.org/10.1038/nmicrobiol.2017.105, 2017.

Linkosalmi, M., Biasi, C., Pumpanen, J., Heinonsalo, J., Lindén, A., Minkkinen, K., ... and Lohila, A. Can the contrasting carbon balances of forestry-drained peatlands be explained by different priming effects?. In International Peat Congress (pp. Article-No). International Peat Society., 2012.

675 Litaor, M. I., Reichmann, O., Belzer, M., Auerswald, K., Nishri, A., and Shenker, M. Spatial analysis of phosphorus sorption capacity in a semiarid altered wetland. Journal of Environmental Quality, 32(1), 335-343., https://doi.org/10.2134/jeq2003.3350, 2003.

Litaor, M. I., Reichmann, O., and Shenker, M. Genesis, classification and human modification of peat and mineral-organic soils, Hula Valley, Israel. Mires and Peat, 9., https://doi.org/10.19189/MaP.2011.OMB.116, 2011.

680 Lützow, M. v., Kögel-Knabner, I., Ekschmitt, K., Matzner, E., Guggenberger, G., Marschner, B., and Flessa, H. Stabilization of organic matter in temperate soils: Mechanisms and their relevance under different soil conditions - a review. European Journal of Soil Science, 57(4), 426--445., https://doi.org/10.1111/j.1365-2389.2006.00809.x, 2006.

Marish. The Hula: A soil survey report (Report, in Hebrew). Israel Ministry of Agriculture / Water Commissioner, 685 Department of Soil Conservation and Drainage, Lake Kinneret Authority., 1986.

Manzoni, S., and Porporato, A. Soil carbon and nitrogen mineralization: Theory and models across scales. Soil Biology and Biochemistry, 41(7), 1355-1379., https://doi.org/10.1016/j.soilbio.2009.02.031, 2009.

Manzoni, S., Piñeiro, G., Jackson, R. B., Jobbágy, E. G., Kim, J. H., and Porporato, A. Analytical models of soil and litter decomposition: Solutions for mass loss and time-dependent decay rates Elsevier BV., https://doi.org/10.1016/j.soilbio.2012.02.029, 2012.

690

Markel, D., Sass, E., Lazar, B., and Bein, A. Biogeochemical evolution of a sulfur-iron rich aquatic system in a reflooded wetland environment (Lake Agmon, northern Israel). Wetlands Ecology and Management, 6, 103-120., https://doi.org/10.1023/A:1008414423821, 1998.

Masiello, C. A., Gallagher, M. E., Randerson, J. T., Deco, R. M., and Chadwick, O. A. Evaluating two experimental
695 approaches for measuring ecosystem carbon oxidation state and oxidative ratio. Journal of Geophysical Research: Biogeosciences, 113(G3), https://doi.org/10.1029/2007jg000534, 2008.

MIGAL - Ministry of Galilee Research Institute. Reports by stations; Hava 1 station. Mop-Zafon site. ., 2023.

Mirabito, A. J., and Chambers, L. G. Quantifying mineral-associated organic matter in wetlands as an indicator of the degree of soil carbon protection Elsevier BV., https://doi.org/10.1016/j.geoderma.2023.116327, 2023.

700 Moore, P. D. The ecology of peat-forming processes: A review Elsevier BV., https://doi.org/10.1016/0166-5162(89)90048-7, 1989.

Moore, T. R., and Knowles, R. The influence of water table levels on methane and carbon dioxide emissions from peatland soils. Canadian Journal of Soil Science, 69(1), 33-38., https://doi.org/10.4141/cjss89-004, 1989.

Nabuurs, G., Mrabet, R., Abu, A., Bustamante, M., Clark, H., Aoki, L., . . . Emmet-Booth, J. P. Agriculture, forestry and
705 other land uses (AFOLU) Cambridge University Press., https://doi.org/10.1017/9781009157926.009, 2023.

Nyberg, M., Black, T. A., Ketler, R., Lee, S. -. -, Johnson, M., Merkens, M., . . . Knox, S. H. Impacts of active versus passive Re-Wetting on the carbon balance of a previously drained bog American Geophysical Union (AGU)., https://doi.org/10.1029/2022jg006881, 2022.

Page, S. E., and Baird, A. J. Peatlands and global change: Response and resilience Annual Reviews.,
710 https://doi.org/10.1146/annurev-environ-110615-085520, 2016.

Ravikovitch, S. The peat soils and enriched organic matter soils of the Hula Valley. Agric. Rep, 1, 23-54., 1945.

Rixen, T., Baum, A., Wit, F., and Samiaji, J. Carbon leaching from tropical peat soils and consequences for carbon balances. Frontiers in Earth Science, 4, https://doi.org/10.3389/feart.2016.00074, 2016.

Roe, S., Streck, C., Beach, R., Busch, J., Chapman, M., Daioglou, V., . . . Lawrence, D. Land-based measures to mitigate
715 climate change: Potential and feasibility by country Wiley., https://doi.org/10.1111/gcb.15873, 2021.

Rowley, M. C., Grand, S., and Verrecchia, É P. Calcium-mediated stabilisation of soil organic carbon Springer Science and Business Media LLC., https://doi.org/10.1007/s10533-017-0410-1, 2017.

Saenger, A., Cécillon, L., Poulenard, J., Bureau, F., De Daniéli, S., Gonzalez, J., and Brun, J. Surveying the carbon pools of mountain soils: A comparison of physical fractionation and rock-eval pyrolysis. Geoderma, 241-242, 279.,
720 https://doi.org/10.1016/j.geoderma.2014.12.001, 2014.

Scanlon, D., and Moore, T. Carbon dioxide production from peatland soil profiles: the influence of temperature, oxic/anoxic conditions and substrate. Soil Science, 165(2), 153-160., https://doi.org/10.1097/00010694-200002000-00007, 2000.

Sebag, D., Verrecchia, E. P., Cécillon, L., Adatte, T., Albrecht, R., Aubert, M., . . . Trombino, L. Dynamics of soil organic matter based on new rock-eval indices. Geoderma, 284, 185., https://doi.org/10.1016/j.geoderma.2016.08.025, 2016.

725 Six, J., Conant, R. T., Paul, E. A., and Paustian, K. Stabilization mechanisms of soil organic matter: implications for C-saturation of soils. Plant and soil, 241, 155-176., https://doi.org/10.1023/A:1016125726789, 2002.

Tsipris, J., and Meron, M. Climatic and hydrological aspects of the Hula restoration project. Wetlands Ecology and Management, 6(2), 91-101., https://doi.org/10.1023/A:1008424518122, 1998.

Tsipris, J., and Meron, M., Orlov-Levin, V. MIGAL -- Galilee Research Institution; Hula monitoring project report. (in 730 Hebrew), 2022.

Tubiello, F. N., Biancalani, R., Salvatore, M., Rossi, S., and Conchedda, G. A worldwide assessment of greenhouse gas emissions from drained organic soils MDPI AG., https://doi.org/10.3390/su8040371, 2016.

Cowgill, U. M. The waters of Merom: A study of Lake Huleh. I. Introduction and general stratigraphy of a 54 m core. ARCHIV FUR HYDROBIOLOGIE, VOL 66, NO 3, P 249-272, 1969. 9 FIG, 1 TAB, 28 REF., 735 https://doi.org/10.1127/archiv-hydrobiol/66/1969/249, 1969.

Wang, Y., Wang, H., He, J. S., and Feng, X. Iron-mediated soil carbon response to water-table decline in an alpine wetland. Nature communications, 8(1), 15972., https://doi.org/10.1038/ncomms15972, 2017.

Wilson, D., Environment, D. B., Change, C., Murdiyarso, D., Page, S. E., Blain, D., . . . Tuittila, E. -. Greenhouse gas emission factors associated with rewetting of organic soils., https://doi.org/10.19189/MaP.2016.OMB.222, 2016.

740 Yaari-cohen, G., paldi, H., moses, G. and harpaz, A.(1971a). A survey of the peat soils in the Hula- valley, Israel, part I). Ministry of agriculture, department of soil conservation and drainage, Kyriat Shemona, israel, 112 pp. (in Hebrew).

Yaari-cohen, G., paldi, C., moses, G. and harpaz, A. (1971b). A survey of the peat soils in the Hula- valley, Israel, part II---Appendices). Ministry of agriculture, department of soil conservation and drainage, Kyriat Shemona, israel, 78 pp. (in Hebrew).

Yu, Z., Loisel, J., Brosseau, D. P., Beilman, D. W., and Hunt, S. J. Global peatland dynamics since the last glacial 745 maximum. Geophysical Research Letters, 37(13), https://doi.org/10.1029/2010gl043584, 2010.

Zou, J., Ziegler, A. D., Chen, D., Mcnicol, G., Ciais, P., Jiang, X., . . . Zeng, Z. Rewetting global wetlands effectively reduces major greenhouse gas emissions. Nature Geoscience, 15(8), 627., https://doi.org/10.1038/s41561-022-00989-0, 2022.